

## Enhanced adhesion with pedestal-shaped elastomeric stamps for transfer printing

Seok Kim, Andrew Carlson, Huanyu Cheng, Seungwoo Lee, Jung-Ki Park et al.

Citation: *Appl. Phys. Lett.* **100**, 171909 (2012); doi: 10.1063/1.4706257

View online: <http://dx.doi.org/10.1063/1.4706257>

View Table of Contents: <http://apl.aip.org/resource/1/APPLAB/v100/i17>

Published by the [American Institute of Physics](http://www.aip.org).

---

### Related Articles

Trench-filled cellular parylene electret for piezoelectric transducer

*Appl. Phys. Lett.* **100**, 262901 (2012)

Microfluidic three-dimensional hydrodynamic flow focusing for the rapid protein concentration analysis

*Biomicrofluidics* **6**, 024132 (2012)

A new type of optical biosensor from DNA wrapped semiconductor graphene ribbons

*J. Appl. Phys.* **111**, 114703 (2012)

Inhomogeneous mechanical losses in micro-oscillators with high reflectivity coating

*J. Appl. Phys.* **111**, 113109 (2012)

Spatio-temporal analysis of tamoxifen-induced bystander effects in breast cancer cells using microfluidics

*Biomicrofluidics* **6**, 024128 (2012)

---

### Additional information on *Appl. Phys. Lett.*

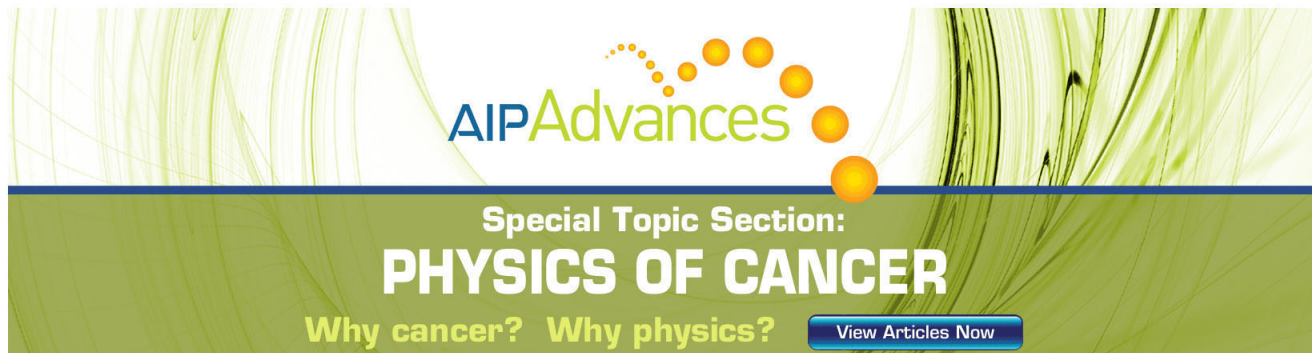
Journal Homepage: <http://apl.aip.org/>

Journal Information: [http://apl.aip.org/about/about\\_the\\_journal](http://apl.aip.org/about/about_the_journal)

Top downloads: [http://apl.aip.org/features/most\\_downloaded](http://apl.aip.org/features/most_downloaded)

Information for Authors: <http://apl.aip.org/authors>

## ADVERTISEMENT

The advertisement features a green and white background with abstract, flowing lines. At the top, the 'AIP Advances' logo is displayed in green and yellow. Below it, the text 'Special Topic Section: PHYSICS OF CANCER' is written in white on a dark green background. At the bottom, the phrase 'Why cancer? Why physics?' is written in yellow, and a blue button with the text 'View Articles Now' is positioned to the right.

AIP Advances

Special Topic Section:  
**PHYSICS OF CANCER**

Why cancer? Why physics? [View Articles Now](#)

## Enhanced adhesion with pedestal-shaped elastomeric stamps for transfer printing

Seok Kim,<sup>1,a)</sup> Andrew Carlson,<sup>1,a)</sup> Huanyu Cheng,<sup>2</sup> Seungwoo Lee,<sup>3</sup> Jung-Ki Park,<sup>3</sup> Yonggang Huang,<sup>2</sup> and John A. Rogers<sup>1,b)</sup>

<sup>1</sup>Department of Materials Science and Engineering, University of Illinois at Urbana-Champaign, 1304 West Green Street, Urbana, Illinois 61801, USA

<sup>2</sup>Department of Civil and Environmental Engineering, Department of Mechanical Engineering, Northwestern University, 2145 Sheridan Road, Evanston, Illinois 61208, USA

<sup>3</sup>Department of Chemical and Biomolecular Engineering, Korea Advanced Institute of Science and Technology, 373-1, Guseong-dong, Yuseong-gu, Daejeon 305-701, Republic of Korea

(Received 17 February 2012; accepted 7 April 2012; published online 25 April 2012)

Microscale elastomeric relief structures with “pedestal” shapes provide enhanced operation in stamps designed for deterministic materials assembly via transfer printing. Experimental measurements of adhesion and finite element analysis both show that for certain geometries, exceptionally large enhancements in adhesion strength (over 15×) can be achieved. Transfer printing of microscale platelets of silicon and ultrathin gallium nitride light emitting diodes onto a silicon substrate without adhesive coatings demonstrates some capabilities in assembly that result from this type of stamp, of interest in diverse applications, including those that involve heterogeneous materials integration. © 2012 American Institute of Physics. [<http://dx.doi.org/10.1063/1.4706257>]

Transfer printing represents a heterogeneous materials assembly and integration strategy, with important applications in classes of electronic and optoelectronic devices that combine rigid inorganic and deformable organic materials.<sup>1–10</sup> The process involves the use of a soft stamp to transfer solid micro/nanostructured materials (i.e., “inks”) from a substrate where they are generated or grown to a different substrate for device integration. In the most versatile form of this procedure, the rate dependent nature of the mechanics of the elastomer used for the stamp allows control of adhesion between it and a structure of interest (i.e., a solid “ink”), where increasing the retraction velocity increases the adhesion.<sup>11</sup> Several other modalities of transfer printing can improve the ability to modulate the adhesion, through the use of microstructured stamps,<sup>12</sup> pressure-controlled contact areas,<sup>13</sup> shear-induced loading techniques,<sup>14</sup> angled relief structures,<sup>15</sup> and laser-assisted thermal transfer.<sup>16</sup> In each case, the goals include strong adhesion when the stamp retrieves an ink from a donor substrate (termed the “adhesion-on” state) and weak adhesion when it releases (i.e., prints) the ink onto a target substrate (termed the “adhesion-off” state). Rectangular posts with flat contacting surfaces represent the most common geometries of relief on a stamp to affect selective retrieval and printing. Although this structure can offer efficient operation for many materials and applications, improved strength of adhesion in the adhesion-on state is often a necessity for advanced printing protocols or for expanded breadth of “printable” materials. None of the previously explored approaches increases the adhesion on-state; modulation is improved, instead, by decreasing the adhesion off-state. One way to enhance adhesion involves modification of the basic rectangular relief geometry (i.e., flat punch) to one that has the shape of a pedestal, using concepts

related to those of fibrillar dry adhesives that adopt the spatula form of gecko foot-hairs.<sup>17–24</sup> Here, we present a design of this general type for enhanced adhesion strength in stamps for transfer printing. Measured contact forces show enhancements of more than 15× with optimized designs, as guided and validated by quantitative modeling of the mechanics.

Figure 1(a) schematically illustrates steps for transfer printing with a pedestal stamp. The advantage of the pedestal design is that it offers enhanced adhesion to the ink, by comparison to a flat punch with similar contact area. As

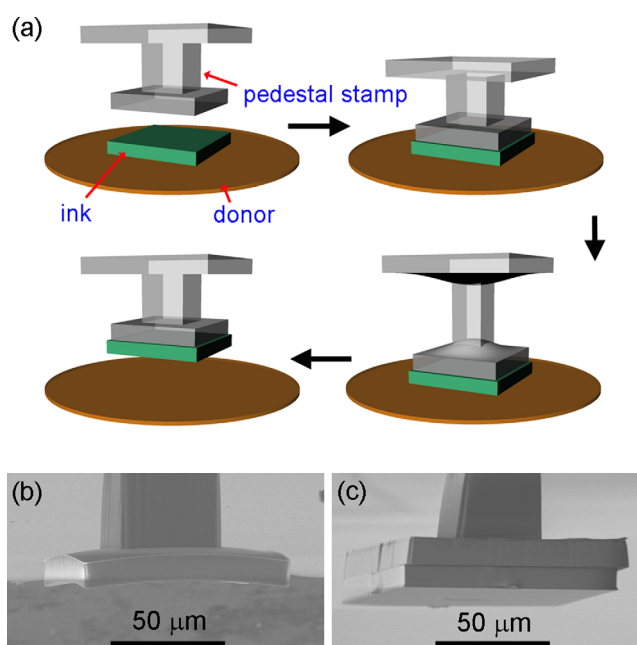


FIG. 1. (a) Schematic illustration of the procedure for transfer printing with a pedestal stamp. SEM images of a stamp with a 50 μm wide post (b) and a 40 μm wide post (c). The latter case has a 100 × 100 μm, 10 μm thick silicon platelet on its surface.

<sup>a)</sup>S. Kim and A. Carlson contributed equally to this work.

<sup>b)</sup>Electronic mail: jrogers@uiuc.edu.

investigated theoretically elsewhere,<sup>24</sup> when subjected to uniform vertical loads, delamination for a flat punch occurs due to cracks that initiate at the external perimeter and propagate toward the center. For a pedestal, crack formation is completely inhibited at the edge and instead initiates at the inner region, usually co-located with the center of the supporting post. For sufficiently clean surfaces, enhanced adhesion is therefore anticipated with a pedestal design due to retarded crack formation and delamination. To explore this system experimentally for transfer printing, we designed and fabricated pedestal features with four different geometries, and characterized their adhesion strength to a flat surface.

The fabrication involved bonding two separate pieces: a thin square pad and a narrow rectangular post on a backing layer, all of which are made of the elastomer polydimethylsiloxane (PDMS, Dow Corning Sylgard 184, 5:1 monomer:crosslinking agent). The bulk of the stamp, comprising the post and backing layer, was formed by molding PDMS against a suitable template structure fabricated by photolithographically patterning a layer of epoxy (SU8 50, MicroChem) on a silicon wafer.<sup>14</sup> For the pedestal pads, an additional template with square trenches ( $100\ \mu\text{m} \times 100\ \mu\text{m}$ ,  $15\ \mu\text{m}$  thick) was created in a similar manner. Here, the PDMS precursor was poured on the template, and the excess scraped away using a razor blade (“doctor blading”) to eliminate material everywhere outside of the recessed square regions.<sup>25</sup> The PDMS precursor in the recessed regions was then partially cured in an oven ( $60\ ^\circ\text{C}$ , 30 min) or on a hot plate ( $110\ ^\circ\text{C}$ , 15 s) to prevent flow due to capillary forces in subsequent steps of stamp fabrication. Next, precision translation and rotation stages and imaging setups were used to contact the prefabricated rectangular post and backing layer with the PDMS precursor in these rectangular trenches, in a co-centered alignment. The combined structure was then cured at  $70\ ^\circ\text{C}$  for  $>1\ \text{h}$  to form strong bonding between the post and the pad. Peeling the integrated structure away from the template completed the fabrication. Figures 1(b) and 1(c) provide scanning electron microscope (SEM) images of pedestal stamps with 50 and  $40\ \mu\text{m}$  thick posts, respectively, both with square cross sections (the stamp with  $50\ \mu\text{m}$  thick post exhibits slight bowing in the pad, likely due to residual stresses that result from the curing procedures). In Figure 1(c), the pedestal stamp holds a  $100\ \mu\text{m} \times 100\ \mu\text{m}$  square,  $10\ \mu\text{m}$  thick silicon platelet, after retrieval from a donor substrate.

The geometries of both the central post and pad have significant influence on the mechanics and resulting adhesive behavior. To quantify the differences for various pedestal designs, a custom setup, described previously,<sup>13,14</sup> was used to measure pull-off forces of the stamp from a flat silicon surface, under vertical loads. The system utilizes a precision load cell (Transducer Techniques, GSO-10) mounted to motorized rotation and  $x$ -,  $y$ -translation stages to provide precise alignment between the load cell and the stamp, the latter of which mounts on an independent  $z$ -stage. For each of the pedestal geometries considered, the contact pad dimensions were fixed ( $100\ \mu\text{m} \times 100\ \mu\text{m} \times 15\ \mu\text{m}$ ) while the rectangular post region linking the pad to the backing layer (Fig. 2(a)) varied in lateral dimensions from 50 to  $100\ \mu\text{m}$ ; the contact areas were the same for all stamps. The results, then, provide

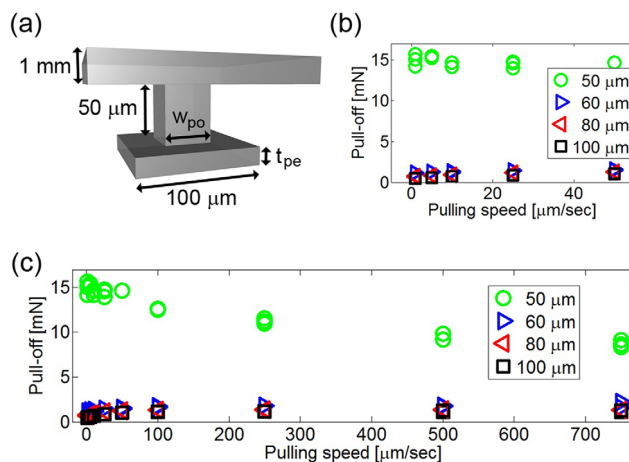


FIG. 2. (a) Illustration of a pedestal stamp, with key dimensions indicated. (b), (c) Pull-off force measured using pedestal stamps with four different post widths, as a function of pulling speed; magnified region at low velocities (b) and for the full range of velocities (c).

insight into the role of the post in concentrating stresses away from the perimeter of pad.

In the testing, a stamp was first brought into contact with a piece of silicon wafer ( $\sim 3\ \text{mm} \times 3\ \text{mm}$ ) connected to the load cell, with a desired applied force (i.e., preload). The stamp was allowed to relax for 5 s while maintaining the compression and then retracted at a fixed velocity. From the recorded force-displacement curves, a maximum pull-off force could be determined, corresponding to the peak value of adhesion for a particular velocity. Figures 2(b) and 2(c) show the velocity-dependent behavior of the pull-off forces for stamps having central posts with several different lateral dimensions. In the case of posts with widths of 60, 80, and  $100\ \mu\text{m}$ , there is a monotonic increase in pull-off force with delamination velocity, consistent with viscoelastic behavior reported for stamps having rectangular surface relief.<sup>14</sup> The similar behaviors in these cases suggest that separation between the stamp and silicon surface is dominated by non-specific van der Waals forces, typical of rate-dependent adhesives like PDMS. Visualization of the stamp at separation with a high-speed camera shows that peeling initiates along one edge of the contact pad and propagates across the stamp/Si interface, consistent with stamps that do not incorporate the pedestal design (e.g., rectangular posts in direct contact with silicon). The results indicate that the central posts in these types of stamps do not sufficiently localize pull-off forces to the center of the contact pad, a condition necessary to initiate interior crack formation. Although the adhesion experiments were conducted against a bare silicon wafer, similar effects of pedestal design on adhesion enhancement are expected with other materials since the geometrical parameters rather than surface chemistry determine the physics.

For a pedestal stamp with a post width of  $50\ \mu\text{m}$ , the pull-off behaviors are qualitatively different from those with larger posts. In this case, the stamp shows strong pull-off forces at low delamination velocities, reaching a maximum peak around  $5\ \mu\text{m}/\text{s}$  and then slowly declining to an approximately constant value. Visualization of the stamp under these slower unloading conditions indicates that peeling

initiates at the center of the contact pad, near the region of the central post, and then propagates outward towards the perimeter, terminating ultimately with complete separation of the stamp and substrate. During retraction, the pad and post undergo extensive deformation before separation, with strains of greater than 150% in the post region alone. These large deformations are consistent with the remarkable adhesive enhancements enabled by these designs, corresponding to a  $15\times$  increase in pull-off force compared to flat punch geometry (e.g.,  $100\ \mu\text{m}\times 100\ \mu\text{m}$ ). For some geometries, the low-velocity adhesive forces are so large that they lead to fracture at the point where the central post meets the backing layer, prior any separation at the contact between the pedestal pad and the substrate. This result indicates that the designs presented here could be limited ultimately by the fracture strength of the PDMS, representing an upper limit to the adhesive strength provided by this material. Effects of vacuum suction are too small to account for the adhesion enhancements observed here, as argued in the context of biological adhesives in other reports.<sup>21,22</sup>

Figure 2(b) shows a magnified region of the measured pull-off forces at low velocities for the four different post widths. Since the material and fabrication methods for all of these cases are the same, the extreme values and different nature of the rate-dependent adhesion are due exclusively to differences in crack initiation and interface separation. By carefully designing the pedestal geometry, stresses can be concentrated to the center of the contact pad, providing a means to drastically increase stamp adhesion without use of complicated surface relief or mechanical loading parameters. We note that the rate-dependent adhesive response of the pedestal geometry with a post width of  $50\ \mu\text{m}$  follows trends that are different from those for the flat punch designs and for other related cases.<sup>14</sup> We speculate that this behavior arises from a complex interaction between the viscoelastic properties of the stamp and the physio-mechanical effects associated with crack initiation in an enclosed region. Further work is needed to establish models that can capture this physics.

The static differences can, on the other hand, be readily understood through three dimensional finite element analysis (3D-FEA) with conditions matched to those used in experiments: pad lateral dimensions of  $100\ \mu\text{m}\times 100\ \mu\text{m}$ , post heights of  $50\ \mu\text{m}$ , and an applied normal direction pull-off force,  $F$ , of 8 mN. The simulations also used a radius of curvature ( $\sim 1\ \mu\text{m}$ ) around the perimeter edge of the contact pad, consistent with the experimental observations. Figures 3(a) and 3(b) show the distribution of normal stress (along the pull-off direction) at the interface between the contact pad and the silicon surface for post widths of 50 and  $60\ \mu\text{m}$ , respectively. The maximum interfacial stress for the  $50\ \mu\text{m}$  post is reached at the central region of the contact pad. In contrast, the  $60\ \mu\text{m}$  post exhibits large stress concentration at the perimeter edges of the pad. These different locations of peak stresses suggest that crack initiation and propagation will start at the center of the interface between the contact pad and silicon for the  $50\ \mu\text{m}$  post and at the edge for the  $60\ \mu\text{m}$  post. The transition from internal to edge cracks occurs between 50 and  $60\ \mu\text{m}$ . This result is further validated by FEA for a  $2\ \mu\text{m}$  internal interfacial crack at the center of

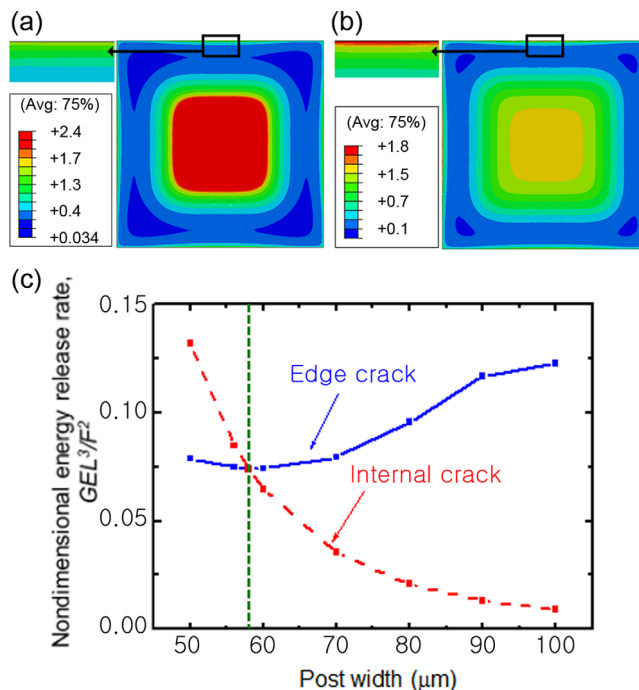


FIG. 3. Distribution of normal stress (along the pull-off direction) at the interface between the contact pad and a silicon surface for post widths of  $50\ \mu\text{m}$  (a) and  $60\ \mu\text{m}$  (b). (c) Interfacial crack tip energy release rates  $G$  versus the post width.

the pad/silicon contact, and by FEA for edge cracks of the same length. Figure 3(c) shows the interfacial crack tip energy release rates  $G$  versus the post width, where  $G$  is normalized by  $F^2/(EL_{\text{pad}}^3)$ ,  $E$  is the Young's modulus of the stamp, and  $L_{\text{pad}}$  is the width of contact pad. The internal crack has a higher energy release rate for post widths of  $50\ \mu\text{m}$  and smaller, whereas the opposite holds for post widths greater than  $60\ \mu\text{m}$ . These results confirm the experimentally observed differences in delamination behavior, indicating that internal and edge crack initiation (and propagation) are responsible for pull-off of pedestal stamps with narrow ( $\leq 50\ \mu\text{m}$ ) and wide ( $\geq 60\ \mu\text{m}$ ) posts, respectively, with a transition that occurs at  $\sim 58\ \mu\text{m}$  (Fig. 3(c)).

Figure 4 provides a demonstration of adhesiveless transfer with pedestal stamps and the suitability for heterogeneous integration. Due to the exceptionally strong adhesive strength that results in this system, we used laser pulses to induce heating and, by differential thermal expansion between the stamp and the ink, delamination, and release.<sup>16</sup> In particular, an infrared (805 nm) laser beam (pulsed at a frequency of 0.2 Hz, with 2.3 ms pulse widths, and peak power of 38 mW) was focused on the pad of a pedestal stamp with an ink on its surface. For the purpose of this demonstration, a  $2\times 2$  array of silicon chips and InGaN microscale inorganic light emitting diodes ( $\mu$ -ILEDs) with lateral dimensions of  $100\ \mu\text{m}\times 100\ \mu\text{m}$  and thicknesses of  $3\ \mu\text{m}$  (silicon) and  $5\ \mu\text{m}$  (InGaN) were printed onto a bare silicon wafer. Figure 4(a) shows an SEM image of the results (the  $\mu$ -ILEDs have square contact pads at opposite corners). To demonstrate that retrieval and printing with a pedestal stamp does not affect performance of the  $\mu$ -ILED, a probe station was used to operate and characterize a representative device.

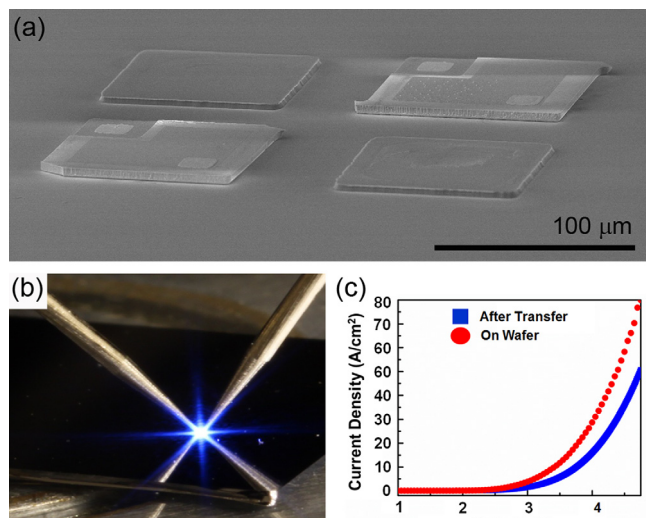


FIG. 4. SEM image of printed Si platelets and microscale InGaN light emitting diodes (a), representative optical image of an operating device (b), and the recorded  $I$ - $V$  characteristics.

Figure 4(b) provides an optical image, while Fig. 4(c) shows the current-voltage ( $I$ - $V$ ) characteristics for such devices before and after printing. The observed current densities are similar to those of devices tested prior to printing and of comparable value to related devices described in the literature.<sup>26</sup>

In summary, the work presented here describes a strategy for greatly increasing the adhesion strength in stamps designed for transfer printing. Finite element mechanics models yield results that are consistent with experimental observation, thereby establishing them as design tools for examining more complex geometries. An interesting opportunity, for example, might involve posts positioned away from the center of the pedestal pad to provide switchable adhesion through control of peel direction. Exploring these possibilities and using the resulting stamps in the fabrication of unusual devices represent topics of current work.

<sup>1</sup>J. Yu and V. Bulović, *Appl. Phys. Lett.* **91**, 043102 (2007).

<sup>2</sup>H. Ko, K. Takei, R. Kapadia, S. Chuang, H. Fang, P. W. Leu, K. Ganapathi, E. Plis, H. S. Kim, S.-Y. Chen, M. Madsen, A. C. Ford, Y.-L. Chueh, S. Krishna, S. Salahuddin, and A. Javey, *Nature* **468**, 286 (2010).

<sup>3</sup>H. Fang, M. Madsen, C. Carraro, K. Takei, H. S. Kim, E. Plis, S.-Y. Chen, S. Krishna, Y.-L. Chueh, R. Maboudian, and A. Javey, *Appl. Phys. Lett.* **98**, 012111 (2011).

<sup>4</sup>L. Sun, G. Qin, J.-H. Seo, G. K. Celler, W. Zhou, and Z. Ma, *Small* **6**, 2553 (2010).

<sup>5</sup>J. Yoon, A. J. Baca, S. I. Park, P. Elvikis, J. B. Geddes, L. Li, R. H. Kim, J. Xiao, S. Wang, T. H. Kim, M. J. Motala, B. Y. Ahn, E. B. Duoss, J. A. Lewis, R. G. Nuzzo, P. M. Ferreira, Y. Huang, A. Rockett, and J. A. Rogers, *Nat. Mater.* **7**, 907 (2008).

<sup>6</sup>S. I. Park, Y. Xiong, R. H. Kim, P. Elvikis, M. Meitl, D. H. Kim, J. Wu, J. Yoon, C. J. Yu, Z. Liu, Y. Huang, K. C. Hwang, P. Ferreira, X. Li, K. Choquette, and J. A. Rogers, *Science* **325**, 977 (2009).

<sup>7</sup>Z. Fan, J. C. Ho, T. Takahashi, R. Yerushalmi, K. Takei, A. C. Ford, Y.-L. Chueh, and A. Javey, *Adv. Mater.* **21**, 3730 (2009).

<sup>8</sup>C. E. Packard, A. Murarka, E. W. Lam, M. A. Schmidt, and V. Bulović, *Adv. Mater.* **22**, 1840 (2010).

<sup>9</sup>Y. Qi, J. Kim, T. D. Nguyen, B. Lisko, P. K. Purohit, and M. C. McAlpine, *Nano Lett.* **11**, 1331 (2011).

<sup>10</sup>S. Guillon, S. Salomon, F. Seichepine, D. Dezest, F. Mathieu, A. Bouchier, L. Mazenq, C. Thibault, C. Vieu, T. Leichlé, and L. Nicu, *Sens. Actuators B* **161**, 1135, (2012).

<sup>11</sup>M. A. Meitl, Z.-T. Zhu, V. Kumar, K. J. Lee, X. Feng, Y. Y. Huang, I. Adesida, R. G. Nuzzo, and J. A. Rogers, *Nat. Mater.* **5**, 33 (2006).

<sup>12</sup>T.-H. Kim, A. Carlson, J.-H. Ahn, S. M. Won, S. Wang, Y. Huang, and J. A. Rogers, *Appl. Phys. Lett.* **94**, 113502 (2009).

<sup>13</sup>S. Kim, J. Wu, A. Carlson, S. H. Jin, A. Kovalsky, P. Glass, Z. Liu, N. Ahmed, S. L. Elgan, W. Chen, P. M. Ferreira, M. Sitti, Y. Huang, and J. A. Rogers, *Proc. Natl. Acad. Sci. U.S.A.* **107**, 17095 (2010).

<sup>14</sup>A. Carlson, H.-J. Kim-Lee, J. Wu, P. Elvikis, H. Cheng, A. Kovalsky, S. Elgan, Q. Yu, and P. M. Ferreira, *Appl. Phys. Lett.* **98**, 264104 (2011).

<sup>15</sup>S. Y. Yang, A. Carlson, H. Cheng, Q. Yu, N. Ahmed, J. Wu, S. Kim, M. Sitti, P. M. Ferreira, Y. Huang, and J. A. Rogers, "Elastomer surfaces with directionally dependent adhesion strength and their use in transfer printing with continuous roll-to-roll applications," *Adv. Mater.* (to be published).

<sup>16</sup>R. Saeidpourazar, R. Li, Y. Li, M. D. Sangid, C. Lü, Y. Huang, J. A. Rogers, and P. M. Ferreira, "Laser-driven micro-transfer placement of pre-fabricated microstructures," *J. Microelectromech.* (to be published).

<sup>17</sup>C. Majidi, R. E. Groff, K. Autumn, S. Baek, B. Bush, N. Gravish, R. Maboudian, Y. Maeno, B. Schubert, M. Wilkinson, and R. S. Fearing, *Phys. Rev. Lett.* **97**, 076103 (2006).

<sup>18</sup>S. Kim and M. Sitti, *Appl. Phys. Lett.* **89**, 261911 (2006).

<sup>19</sup>S. Gorb, M. Varenberg, A. Peressadko, and J. Tuma, *J. R. Soc. Interface* **4**, 271 (2007).

<sup>20</sup>S. Reddy, E. Arzt, and A. del Campo, *Adv. Mater.* **19**, 3833 (2007).

<sup>21</sup>A. V. Spuskanyuk, R. M. McMeeking, V. S. Deshpande, and E. Arzt, *Acta Biomater.* **4**, 1669 (2008).

<sup>22</sup>M. P. Murphy, B. Aksak, and M. Sitti, *Small* **5**, 170 (2009).

<sup>23</sup>H. E. Jeong, J.-K. Lee, H. N. Kim, S. H. Moon, and K. Y. Suh, *Proc Natl. Acad. Sci. U.S.A.* **106**, 5639 (2009).

<sup>24</sup>G. Carbone, E. Pierro, and S. N. Gorb, *Soft Matter* **7**, 5545 (2011).

<sup>25</sup>M. J. Kim, J. Yoon, S.-I. Park, and J. A. Rogers, *Appl. Phys. Lett.* **95**, 214101 (2009).

<sup>26</sup>H. Kim, E. Brueckner, J. Song, Y. Li, S. Kim, C. Lu, J. Sulkin, K. Choquette, Y. Huang, R. G. Nuzzo, and J. A. Rogers, *Proc. Natl. Acad. Sci. U.S.A.* **108**, 10072 (2011).